We are IntechOpen,
the world's leading publisher of
Open Access books
Built by scientists, for scientists

4,800
Open access books available

122,000
International authors and editors

135M
Downloads

Our authors are among the

154
Countries delivered to

TOP 1%
most cited scientists

12.2%
Contributors from top 500 universities

CLARIVATE ANALYTICS
BOOK CITATION INDEX
INDEXED

WEB OF SCIENCE™

Selection of our books indexed in the Book Citation Index
in Web of Science™ Core Collection (BKCI)

Interested in publishing with us?
Contact book.department@intechopen.com

Computation of Hydro-geomorphologic Changes in Two Basins of Northeastern Greece

Konstantinos Kaffas and Vlassios Hrissanthou

Additional information is available at the end of the chapter

Abstract

This chapter presents a composite mathematical model aiming at continuous simulations of hydro-geomorphological processes at the basin scale. Continuous hydrologic simulations, as well as continuous simulations of soil and streambed erosion processes, are performed in two neighbouring basins in northeastern Greece: Kosynthos river basin (district of Xanthi, Thrace, northeastern Greece) and Nestos river basin (Macedonia-Thrace border, northeastern Greece). Both basins are mountainous and covered by forested and bushy areas in their greatest part. Kosynthos river basin extends to an area of 237 km², whilst Nestos river basin is quite bigger, covering an area of approximately 840 km². The characteristic of Nestos river basin is the presence of a dam at its northwestern boundary, which largely affects the discharge, as well as the sediment transport in Nestos River. The application of the model results in continuous hydrographs and sediment graphs at the outlets of the two basins. Fine temporal scales are used, providing this way a continuous assessment of water and sediment discharge. The statistic efficiency criteria utilized for the comparison between computed and measured values of water and sediment discharge at the basin outlet provide satisfactory results. Therefore, it is concluded that the continuous hydro-geomorphologic modelling can be successfully applied to Kosynthos and Nestos river basins.

Keywords: hydro-geomorphology, continuous hydrographs, soil erosion, sediment transport, continuous sediment graphs, sediment yield

1. Introduction

Hydro-geomorphology is primarily a matter of water and sediment. This constitutes the study of hydrological processes, as well as of the soil and streambed erosion processes, imperative. Surface runoff, baseflow, stream discharge, soil erosion and sediment transport constitute the

basic interrelated natural processes, which perpetually chisel the geomorphological profile of a basin. In most cases, it takes hundreds or even thousands of years for any effect to take its toll on the geomorphological profile of the earth. However, it is worth studying the hydro-geomorphological processes at a continuous timescale. Apart from the quantification of the hydrological processes, as well as of the soil and streambed erosion processes, the continuous hydro-geomorphologic modelling provides valuable information for the future trend of these physical processes.

There is a wide variety of integrated models that continuously simulate the runoff, soil erosion and sediment transport processes. Just a few of these models are listed below. Most of these models are available in their software form:

1.1. Areal non-point source watershed environment response simulation model (ANSWERS)

ANSWERS [1] is a physically based, distributed model. Although the model was initially developed to operate on an event basis, it underwent modifications to be used for continuous simulations as well [2]. The current version of ANSWERS can continuously simulate runoff by means of the Holtan [3] or the Green and Ampt infiltration methods [4]. The continuity equation is the basic equation used for the computation of surface runoff:

$$\frac{dS}{dt} = I - O \tag{1}$$

where S is the volume of water in storage (surface detention), t is the time, I is the inflow rate and O is the outflow rate.

Soil erosion is modelled by estimating raindrop detachment using rainfall intensity and universal soil loss equation (USLE) factors [5]. As far as sediment transport is concerned, Yalin's bed load transport equation is used [6]:

$$T = 146 \cdot s \cdot Q^{\frac{1}{2}} \quad \text{for } Q \leq 0.046 \, [\, m^3/(\min m) \,] \tag{2}$$

$$T = 14,600 \cdot s \cdot Q^2 \quad \text{for } Q \geq 0.046 \, [\, m^3/(\min m) \,] \tag{3}$$

where T is the transport capacity by surface runoff [kg/(min m)], s is the surface slope and Q is the flow rate per unit width [m³/(min m)].

Yalin's equation was originally conceived for the routing of sediments through a channel. However, several attempts have been made towards the application of this channel formula for overland flow. Amongst these, Foster and Meyer [7], as well as Alonso et al. [8], proved that Yalin's equation can successfully be applied for sediment transport by surface runoff.

1.2. Agricultural non-point source model (AGNPS)

AGNPS [9, 10] is a conceptual distributed model, which operates on a cell basis. AGNPS was also initially developed for event-based simulations. Latest versions of the model, though, offer the ability for long-term hydrologic and soil erosion simulations. The modelling of runoff is based on soil conservation service (SCS)-curve number (CN) method [11] (Section 4.1).

Soil erosion and sediment transport on the soil surface are modelled using the revised universal soil loss equation (RUSLE) [12]:

$$A = R \cdot K \cdot L \cdot S \cdot C \cdot P \tag{4}$$

where A is the average soil loss per unit area and time [t/(ha yr)], R is the rainfall erosivity factor [MJ mm/(ha h yr)], K [t h/(MJ mm)] is the soil erodibility factor, L is the slope length factor, S is the slope steepness factor, C is the cover and management factor and P is the support practice factor.

The RUSLE is exactly the same with USLE. The only difference between RUSLE and USLE is that the factors K, L, S, C and P, in RUSLE, are computed in more detail.

Sediment routing in streams is modelled by a modified Einstein deposition equation [13] and the Bagnold suspended sediment formula for stream sediment transport [14].

1.3. Chemical runoff and erosion from agricultural management systems model (CREAMS)

Another physically based model which can continuously simulate the hydro-geomorphological processes, at the basin scale, is the chemical runoff and erosion from agricultural management systems model (CREAMS) [15]. As in the case of AGNPS, runoff modelling in CREAMS is based on the SCS-CN method for the estimation of hydrologic losses due to infiltration and kinematic surface water flow equations. The peak runoff rate is computed by the following equation:

$$q_{\mathrm{p}} = 200 \, (DA)^{0.7} \cdot (CS)^{0.15} \cdot Q^{0.917(DA)^{0.0166}} \cdot (LW)^{-0.187} \tag{5}$$

where q_{p} is the peak runoff rate (m³/s), DA is the drainage area (km²), CS is the channel slope, Q is the daily runoff volume (mm) and LW is the length-width ratio of the basin.

The erosion component maintains elements of the USLE but includes sediment transport capacity for overland flow, which is estimated by the steady-state continuity equation:

$$\frac{d\,q_{\mathrm{s}}}{dx} = D_{\mathrm{L}} + D_{\mathrm{F}} \tag{6}$$

where q_{s} is sediment discharge per unit width [kg/(s m)], x is the distance downslope (m), D_{L} is the lateral inflow of sediment [kg/(s m²)] and D_{F} is the detachment or deposition of sediment by flow [kg/(s m²)].

The composite mathematical model (CMM), applied in this study, comprises three sub-models: a rainfall-runoff submodel, a submodel for the simulation of soil erosion and a sediment transport submodel for the routing of sediments in streams. The rainfall-runoff submodel that is used for the computation of the overland flow, as well as of the flow in the mainstreams of the sub-basins, is the conceptual, semi-distributed hydrologic model HEC-HMS 4.2. The soil erosion submodel, utilized for the estimation of soil erosion in a sub-basin, is based on the relationships of Poesen [16]. The estimate of sediment yield at the outlet of a sub-basin, and finally at the outlet of the whole basin, is achieved by means of the stream sediment transport model of Yang and Stall [17]. The CMM was applied to Kosynthos river basin and to Nestos river basin. The application of all three models results

in continuous hydrographs and sediment graphs at the basin outlet. The computed stream discharge and sediment discharge values are compared with field measurements, and all models are evaluated as to their competence of simulating the hydro-geomorphological processes in a basin.

The geomorphology of the earth's surface is shaped by physical, chemical, biological as well as geological processes. This chapter focuses on the effect that the physical processes have on the geomorphological profile of a soil surface. The component of physical processes mainly refers to the hydro-geomorphological processes.

2. Description of the study area

2.1. Kosynthos river basin

Kosynthos River originates from Mount Erymanthos in the mountain chain of central Rodopi, flows in a southeastern course, passes through the city of Xanthi and empties in Vistonida Lake close to the ancient city of Anastasioupoli. Its overall length is approximately 55 km. The study area concerns the mountainous part of the basin and extends to 237 km^2 (**Figure 1**) from the Greek-Bulgarian border, to the North, to the city of Xanthi and to the South and from the mountainous region of Livaditis, to the East, to the mountainous region between Myki and Kentavros and to the West. The altitude varies between 72 m and 1700 m, the average land
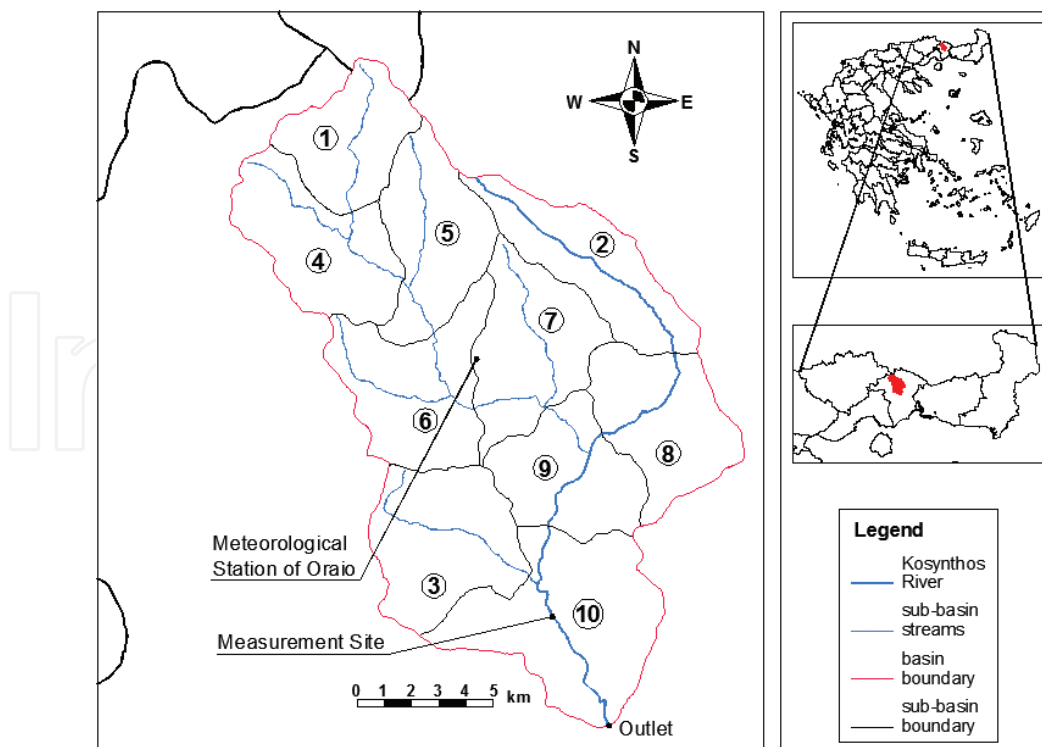

Figure 1. Kosynthos river basin.

slope of the basin is 37.3% and the length of the part of Kosynthos River that runs the basin is approximately 35 km.

The climate of the study area is of temperate Mediterranean type where the average annual temperature is 14°C and annual precipitation is about 750 mm.

The basin of Kosynthos River consists of forests (74%), bushes (4.5%), urban area (1.5%) and an area with no significant vegetation (sparse vegetation) (20%). The dominant rocks are granite-diorite, marble, gneiss-granite and migmatite. The structure of the semi-permeable soil in combination with the structure of the bedrock, which has a low percentage of deep percolation, favours a relatively high runoff discharge.

2.2. Nestos river basin

Nestos River straddles the border between Macedonia and Thrace in northeastern Greece (**Figure 2**). The study area of Nestos river basin falls in the Greek mountainous part downstream of Platanovrysi dam, which is located on the Macedonian-Thrace border, in northeastern Greece (**Figure 2**). The area of the basin is approximately 840 km². The altitude varies between 38 m and 1747 m, the average land slope of the basin is 37% and the length of the part of Nestos River that runs the basin is approximately 63 km.

The Platanovrysi dam (**Figure 2**) is operated by the Hydroelectric Power Production Agency of Hellenic Public Electricity Corporation. The daily dam discharges were provided by the
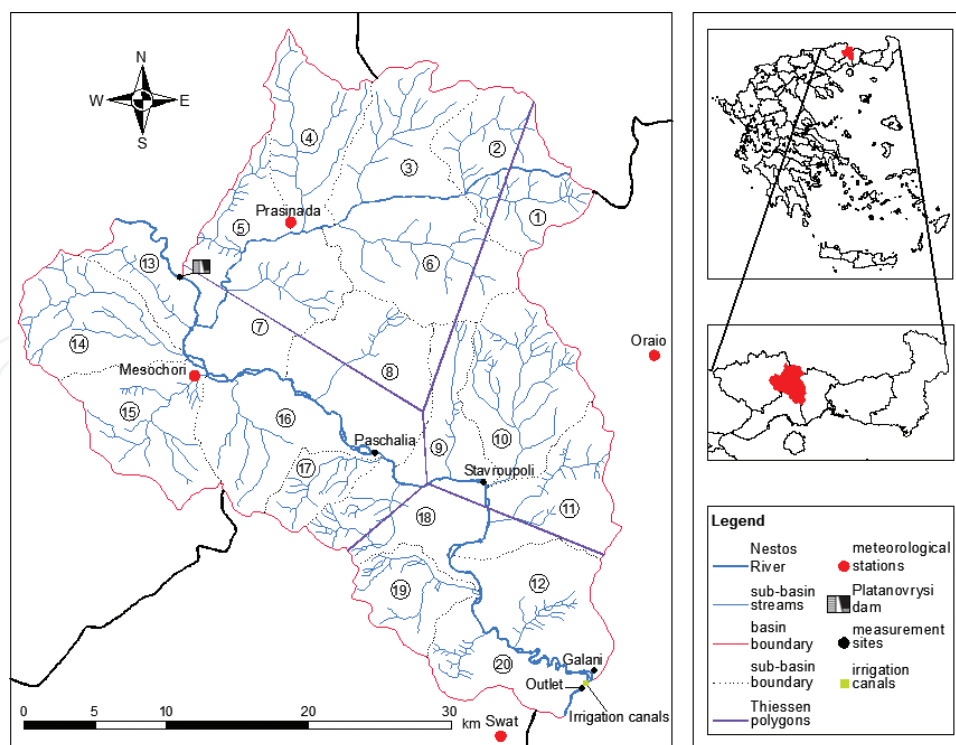

Figure 2. Nestos river basin.

Hydroelectric Power Production Agency for the entire study period (11 September 2005–31 July 2014). The two irrigation canals (**Figure 2**) are located at the left and right banks of the same cross-sectional area, very close to the Egnatia bridge of Nestos River, just slightly upstream of the basin outlet. The irrigation canals are operated by the local land reclamation agencies of Thalassia-Kremasti and Chrysoupoli. The irrigation season starts in the middle of April and goes up to the end of October; in some cases, it extends up to early November also.

The land cover data in combination with the soil permeability data are represented by the CN. The study area under investigation is covered mostly by forested and bushy areas and followed by crops, whilst a very small portion falls under urban areas and areas with no significant vegetation.

Soil texture data were obtained from soil associations' maps and were provided from Ref. [18]. There are four dominant soil types of the basin mainly: sandy clay loam (sand 55%, clay 19% and silt 26%), silty loam (sand 22%, clay 21% and silt 57%), loamy sand (sand 78%, clay 4% and silt 18%) and silty clay loam (sand 8%, clay 39% and silt 53%).

The bedrock mainly consists of semi-permeable rocks which do not favour deep percolation. The dominant rocks are marble, aluminous schist, rhyolite, lignite, schist, granite, granite-diorite, gneiss and gneiss-granite.

3. Meteorological data and field measurements

3.1. Kosynthos river basin

There is only one available meteorological station in the area of investigated part of Kosynthos river basin which has the data available from 1 January 2005 to 15 March 2009 (**Figure 1**). The meteorological data used for the application of the model are the following: rainfall depth (mm), minimum, maximum and average daily temperatures (°C), atmospheric pressure (kPa), wind speed at 2 m height (m/s) and solar radiation [MJ/(m^2 day)]. All of the aforementioned meteorological data were used at a daily time step for modelling. The meteorological station of Oraio is placed at the very centre of the basin (**Figure 1**), at an elevation of 800 m. Nonetheless, the rainfall data of only one meteorological station are neither sufficient nor representative of the whole basin, especially for the sub-basins close to the basin outlet.

The Laboratory of Hydrology and Hydraulic Structures, Civil Engineering Department, Democritus University of Thrace carried out 38 discharge measurements near the outlet of Kosynthos river basin, 5 of which in October, November and December 2005, 10 in March, April, May, June and July 2006, 14 in March, April and May 2007, 8 in May, June, July, September, November and December 2008 and 1 in January 2009. Additionally, 28 measurements of bed load and suspended load were carried out near the outlet of Kosynthos river basin, 4 of which in November, December 2005, 9 in March, April, May and June 2006, 6 in

April and May 2007, 8 in May, June, July, September, November and December 2008 and 1 in January 2009 (**Figure 1**).

Measurements of bed load transport and suspended load transport were carried out at the same time as the stream discharge measurements.

3.2. Nestos river basin

There are four meteorological stations in the Nestos river basin. Two of the stations are located inside the basin and the other two are little out of it (**Figure 2**). The data from the stations Mesochori and Prasinada, which lie inside the basin, were provided by the Hydroelectric Power Production Agency, the meteorological station of Oraio is operated by the Civil Engineering Department of Democritus University of Thrace, whilst the data from Soil and Water Assessment Tool (SWAT) station were obtained from the internet site Global Weather Data for SWAT [19] and were provided by the Ecosystem Sciences and Management Department of Texas A&M University, the USA. The meteorological data obtained from the meteorological stations are the rainfall depth (mm), minimum, maximum and average values of temperature (°C), wind speed (m/s), relative humidity and solar radiation (W/m²). All these meteorological data are used at a daily time step. The distribution of the meteorological stations to areas of influence was achieved with Thiessen polygons [20] (**Figure 2**).

About 143 discharge measurements were carried out by the Laboratory of Hydrology and Hydraulic Structures of Civil Engineering Department, Democritus University of Thrace and the Laboratory of Ecological Engineering and Technology of Environmental Engineering Department, Democritus University of Thrace at four different intersections of the Nestos River—Paschalia, Stavroupoli, Galani and the basin outlet (**Figure 2**). These measurements were taken from September 2005 to May 2011, not on a regular basis. However, all months are covered through the above period. Moreover, the Laboratory of Hydrology and Hydraulic Structures carried out 40 measurements of bed load and suspended load at the outlet of the basin (**Figure 2**). Five of these measurements were carried out in September 2005 (**Figure 16**), whilst the rest from June 2008 to June 2011 (**Figure 17**).

4. Theoretical description of the composite mathematical model

4.1. Rainfall-runoff submodel

The purpose of the rainfall-runoff submodel is to simulate and quantify all the natural processes, taking place when rainfall starts, and to lead to the final transformation of rainfall-to-runoff hydrograph. The rainfall-runoff submodel consists of several components, each describing a natural process. These components are the rainfall excess, the evapotranspiration, lag time and time of concentration and the transformation of rainfall excess into runoff hydrograph. Since, in this case, we are interested in the simulation of the stream sediment

transport processes as well, a flood routing model and a baseflow model are added. The basic equations of these methods are given below.

4.1.1. Rainfall excess model

The SCS-CN (NRCS since 1994) is used for the estimation of the hydrologic losses due to infiltration as well as for the estimation of rainfall excess [11]. The amount of rainfall excess is transformed into surface runoff.

$$Q = \frac{(P - 0.2S)^2}{P + 0.8S} \quad \text{for } P > 0.2S, \text{ otherwise } Q = 0 \tag{7}$$

where Q is the rainfall excess (mm), P is the total rainfall (mm) and S is the maximum hydrologic losses (mm).

4.1.2. Evapotranspiration

For estimating the potential evapotranspiration, ET_o (mm/day), the widely known Penman-Monteith FAO-56 equation was used [21]:

$$E T_o = \frac{0.408\Delta(R_n - G) + \gamma \frac{900}{T + 273} u_2(e_s - e_a)}{\Delta + \gamma(1 + 0.34 u_2)} \tag{8}$$

where R_n is the net radiation at the crop surface [MJ/(m^2 day)], G is the soil heat flux density [MJ/(m^2 day)], T is the mean daily air temperature at height ranging from 1.5 m to 2.5 m (°C), u_2 is the wind speed at 2 m height (m/s), e_s is the saturation vapour pressure at height ranging from 1.5 m to 2.5 m (kPa), e_a is the actual vapour pressure at height ranging from 1.5 m to 2.5 m (kPa), Δ is the slope of the vapour pressure curve (kPa/°C) and γ is the psychrometric constant (kPa/°C).

4.1.3. Lag time and time of concentration

Lag time is calculated by means of the empirical equation of SCS [11]. SCS relates lag time, t_p, with the time of concentration, t_c:

$$t_p = 0.6 t_c \tag{9}$$

Various equations are available for the estimation of the concentration time. In the present study, the most suitable was found to be Giandotti's formula [22, 23], for Kosynthos river basin, and Pasini's formula [24], for Nestos river basin.

4.1.4. Transformation of rainfall excess into runoff hydrograph

The transformation of rainfall excess into runoff hydrograph is achieved by means of the dimensionless synthetic unit hydrograph of soil conservation service [25].

4.1.5. Baseflow method

The applied rainfall-runoff submodel includes an exponential recession model to represent the time variation of baseflow [26] (**Figure 3**).
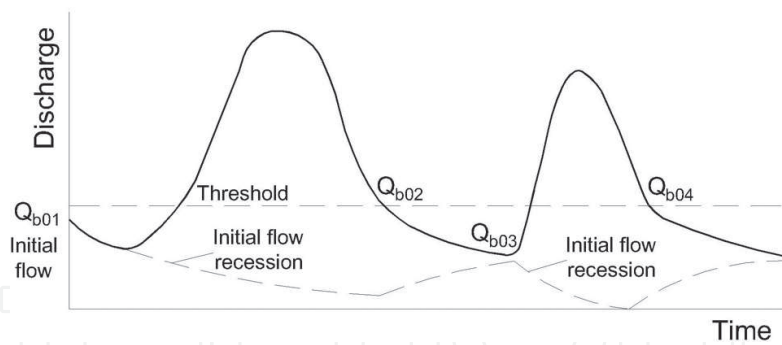
Figure 3. Recession with multiple runoff peaks.

The baseflow recession model can be described by Eq. (10).

$$Q_{bt} = Q_{b0} k^t \tag{10}$$

where Q_{bt} is the baseflow at any time t, Q_{b0} is the initial baseflow (at time zero) and k is the exponential decay constant; it is defined as the ratio of the baseflow at time t to the baseflow one day earlier.

4.1.6. Routing model

For the routing of the total discharge (direct runoff + baseflow) hydrograph in the main streams of the basin, the Muskingum-Cunge model is used. The Muskingum-Cunge model is based on the widely used hydrologic routing Muskingum model [27].

The aforementioned methods are incorporated and are given as options in the "sub-basin" and "reach" editors in the hydrologic model HEC-HMS 4.2 [28]. The result from HEC-HMS is the development of runoff, baseflow and total discharge hydrographs.

A more thorough outline of the rainfall-runoff submodel can be found in Ref. [29].

4.2. Soil erosion submodel

The objective of this submodel is to estimate the sediment yield that results from the erosion of the soil surface and reaches the main streams of the sub-basins. This is done by calculating firstly the amount of soil detachment by rainfall (detachment by raindrop impact) and secondly the amount of soil erosion due to surface runoff (shearing force of flowing water).

The estimation of soil erosion due to rainfall was performed by means of Poesen's relations [16]:

$$q_{rs} = C(KE) r_s^{-1} \cos a \tag{11}$$

$$q_r = q_{rs} [\, 0.301 \sin a + 0.019 \, D_{50}^{-0.22}(1 - e^{2.42 \sin a}) \,] \tag{12}$$

where q_{rs} is the mass of detached particles per unit area (kg/m²), C is the soil cover factor, KE is the rainfall kinetic energy (J/m²), r_s is the soil resistance to drop detachment (J/kg), a is the slope gradient (°), q_r is the downslope splash transport per unit width (kg/m) and D_{50} is the median particle diameter (m).

The soil erosion due to runoff is calculated using Nielsen's relation [30]:

$$q_f = r_e q_t \tag{13}$$

where q_f is the sediment transport per unit width by runoff [m³/(s m)], r_e is the entrainment ratio ($r_e = 1$ for non-cohesive soils, $r_e < 1$ for cohesive soils) and q_t is the sediment transport capacity per unit width by runoff [m³/(s m)].

For the surface runoff sediment transport capacity, q_t, the modified formula of Engelund-Hansen is used [31]:

$$q_t = 0.04 \frac{(2g/f)^{1/6}}{[(\rho_s/\rho - 1)^2 g^{1/2} D_{50}]} q^{5/3} s^{5/3} \tag{14}$$

The sediment yield that reaches the stream is calculated by means of comparison between the available sediment and the sediment transport capacity by runoff [32].

4.3. Sediment transport submodel for streams

The final stage in the hydro-geomorphological modelling is the routing of sediments into the main streams. This is done on the basis of the comparison between the sediment transport capacity by streamflow and the available sediment in the stream. The available sediment in the stream is the sediment yield that was calculated by the soil erosion submodel. This comparison between sediment transport capacity by streamflow and the available sediment in the stream defines whether erosion or deposition takes place in the stream.

Sediment transport capacity by streamflow is estimated from the sediment concentration in the stream, which is computed by the unit stream power model of Yang and Stall [17]:

$$\log c_{ts} = 5.435 - 0.286 \log \frac{w D_{50}}{v} - 0.457 \log \frac{u_*}{w}$$
$$+ \left(1.799 - 0.409 \log \frac{w D_{50}}{v} - 0.314 \log \frac{u_*}{w}\right) \log\left(\frac{us}{w} - \frac{u_{cr} s}{w}\right) \tag{15}$$

$$\frac{u_{cr}}{w} = \frac{2.5}{\log(u_* D_{50}/v - 0.06)} + 0.66, \quad \text{if } 1.2 < \frac{u_* D_{50}}{v} < 70 \tag{16}$$

$$\frac{u_{cr}}{w} = 2.05, \quad \text{if } \frac{u_* D_{50}}{v} \geq 70 \tag{17}$$

where c_{ts} is the total sediment concentration by weight (ppm), w is the terminal fall velocity of sediment particles (m/s), D_{50} is the median particle diameter (m), v is the kinematic viscosity of the water (m²/s), s is the energy slope, u is the mean flow velocity (m/s), u_{cr} is the critical mean flow velocity (m/s) and u_* is the shear velocity (m/s).

5. Application and calibration of the model

Once all the necessary data have been gathered and processed, the model is applied. This is the first essential step of modelling. This procedure should be followed by the calibration of the model and finally by its validation. The integrated procedure is schematically described in **Figure 4**.
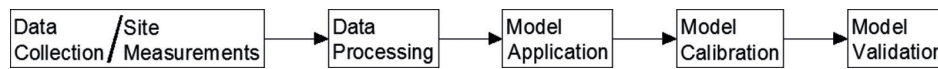
Figure 4. Schematic representation of modelling process.

5.1. Kosynthos river basin

The hydrologic model was applied for the data period of 2005–2009, that is from 1 January 2005 to 15 March 2009, in HEC-HMS 4.2. The resulting runoff, baseflow and total discharge hydrographs, from HEC-HMS, along with the rainfall amount, were used as the decisive input data to the soil erosion model, the outcome of which is the sediment inflow to main streams. Subsequently, the sediment available in the main streams, in combination with the sediment transport capacity of the main streams, determines the final sediment yield at the outlet of the basin.

The continuous nature of the hydrograph enables the development of a continuous sediment graph. For more precise calculations, the basin was divided into 10 natural sub-basins (**Figure 1**).

All the submodels of the composite mathematical model were calibrated. A simple calibration procedure was followed. All submodels ran with the calibrated parameters starting with their initial values. For every new run of the CMM, the calibrated parameters reentered the submodels with a changed value. This procedure was applied repeatedly until computations and measurements reached the best possible agreement. The calibrated parameters are shown in **Table 1**. The numbers in brackets refer to either the percentage change or the final value obtained by the parameters, whilst the numbers in parentheses refer to the times that each parameter has been reentered in the model, with a changed value, during the calibration process.

Recession constant and threshold discharge are two parameters used in HEC-HMS to reset baseflow during a rainfall event. These two parameters are very crucial, as they greatly regulate baseflow and, therefore, total stream discharge.

The recession constant describes the rate at which baseflow recedes between storm events. It is defined as the ratio of baseflow at the current time to the baseflow 1 day earlier.

The entrainment ratio defines the cohesion of the soil and has been described in Section 4.2 [Eq. (13)].

Roughness coefficient is a parameter that greatly affects the transport capacity by streamflow and, hence, the final sediment discharge at the basin outlet.

Parameters that cannot be directly measured, in comparison with parameters that are measurable (rainfall depth, water discharge, meteorological data, etc.), are best suited for calibration. Such parameters, amongst others, can be the calibrated parameters in **Tables 1** and **2**, namely: curve number, lag time, baseflow recession constant, flow ratio, entrainment ratio and streambed roughness. Nevertheless, all parameters were considered for calibration within a reasonable range to ensure these do not lose their physical meaning.

5.2. Nestos river basin

For the needs of modelling, the basin was divided into 20 natural sub-basins (**Figure 2**). The model was applied separately for four different cases. For each case, each one of the four measurement sites (Paschalia, Stavroupoli, Galani, basin outlet) (**Figure 2**) was considered as the outlet of the basin. This implies the exemption of several sub-basins, for example, the case of Paschalia and Stavroupoli.

The difference between the simulations for Galani and the basin outlet is that Galani is located upstream of the irrigation canals, whilst the outlet of the basin is located slightly downstream. Hence, in the case of the basin outlet, the discharge allocated for irrigation was extracted from the total discharge, during the irrigation periods.

The discharges of Platanovrysi dam were inputted at a daily time step in HEC-HMS. As far as the operation of HEC-HMS is concerned, the dam is regarded as a source point.

Submodels	Calibrated parameters			
Rainfall-runoff submodel	CN	Lag time	Baseflow recession constant	Flow ratio
	[+5%]	[−3%]	[0.9]	[0.27]
	(7)	(6)	(4)	(4)
Soil erosion submodel (relationships of Poesen)	Entrainment ratio			
	[0.65]			
	(6)			
Stream sediment transport submodel	Streambed roughness			
	[−10%]			
	(8)			

Table 1. Calibrated parameters for Kosynthos river basin.

Submodels	Calibrated parameters			
Rainfall-runoff submodel	CN	Lag time	Baseflow recession constant	Flow ratio
	[−8%]	[+10%]	[0.81]	[0.16]
	(9)	(8)	(6)	(6)
Soil erosion submodel (relationships of Poesen)	Entrainment ratio			
	[0.7]			
	(8)			
Stream sediment transport submodel	Streambed roughness			
	[+15%]			
	(6)			

Table 2. Calibrated parameters for Nestos river basin.

All the simulations for Nestos river basin cover a period from 11 September 2005 to 31 July 2014.

A multi-site calibration procedure was implemented for Nestos river basin. The two upstream measurement sites, of Paschalia and Stavroupoli, were used for calibration of the model, whilst the measurements of the two downstream measurement sites, of Galani and the basin outlet, were used for the validation of it. The calibrated parameters are the same with those for Kosynthos river basin and are shown in **Table 2**. At this point, it has to be noted that the calibration of the CMM was dealt with two different objectives for the two basins. This explains the different values obtained by the calibrated parameters in **Tables 1** and **2**. For instance, the increase of discharge was sought in the case of Kosynthos river basin, whilst for Nestos river basin the decrease of discharge was intended.

6. Results: model validation

6.1. Kosynthos river basin

6.1.1. Water discharge

In **Figure 5**, the computed discharge hydrograph (direct runoff + baseflow) and the measured discharge values at the basin outlet are depicted for the period October 2005–March 2009.

Discharge is mainly driven by rainfall. This means that in high rainfall seasons there is a discharge increase. From the above hydrograph, the months with the highest rainfall depths and discharges are March, October, November and December.

6.1.2. Sediment discharge

In **Figures 6–8**, the computed sediment graphs (bed load + suspended load) at the basin outlet are illustrated for the periods October 2005–July 2006, April–May 2007 and April 2008–January 2009.
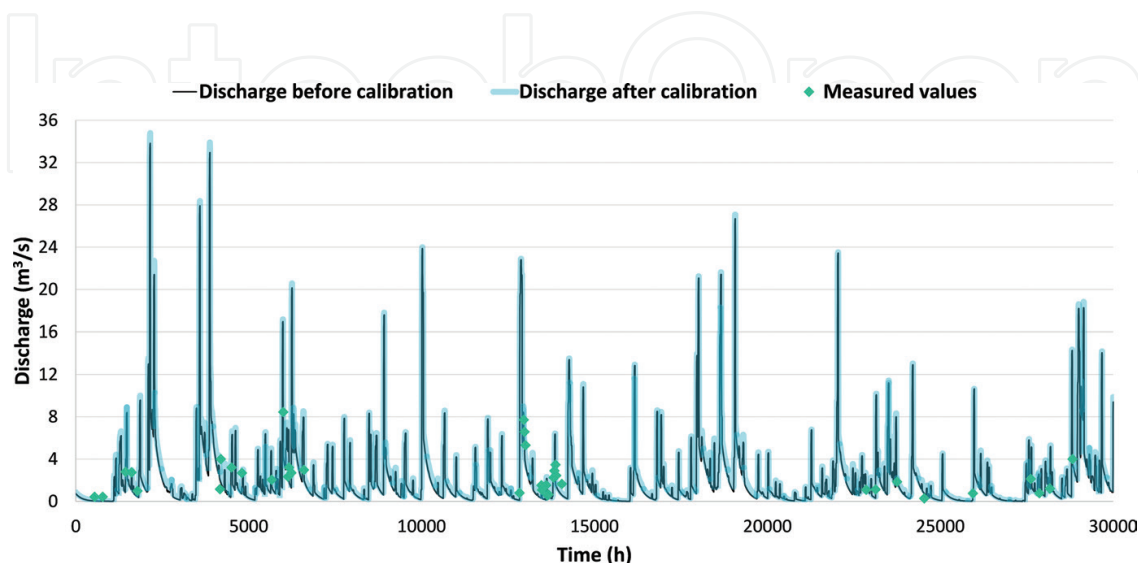

Figure 5. Discharge hydrograph (October 2005–March 2009, Kosynthos river basin outlet).
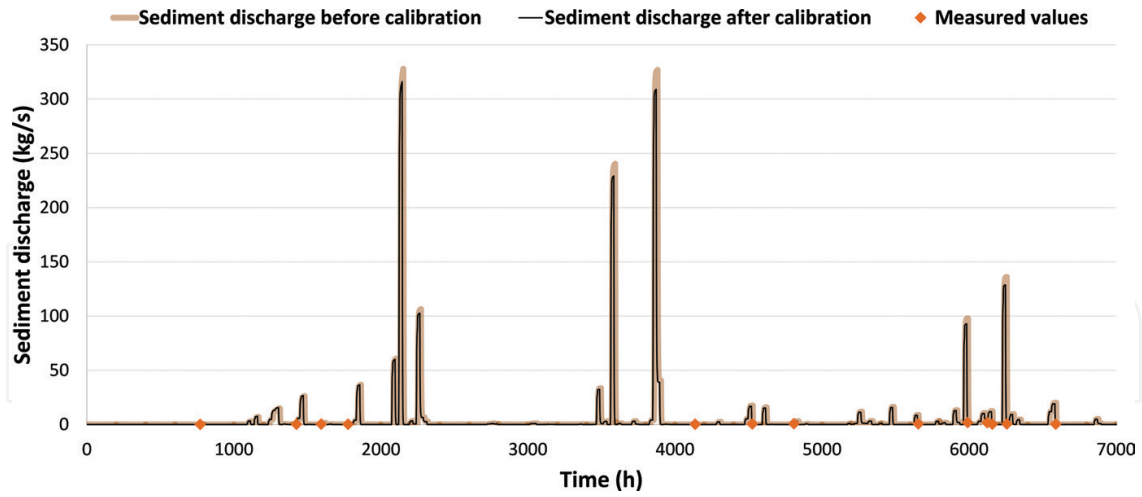
Figure 6. Sediment graph (October 2005–July 2006, Kosynthos river basin outlet).
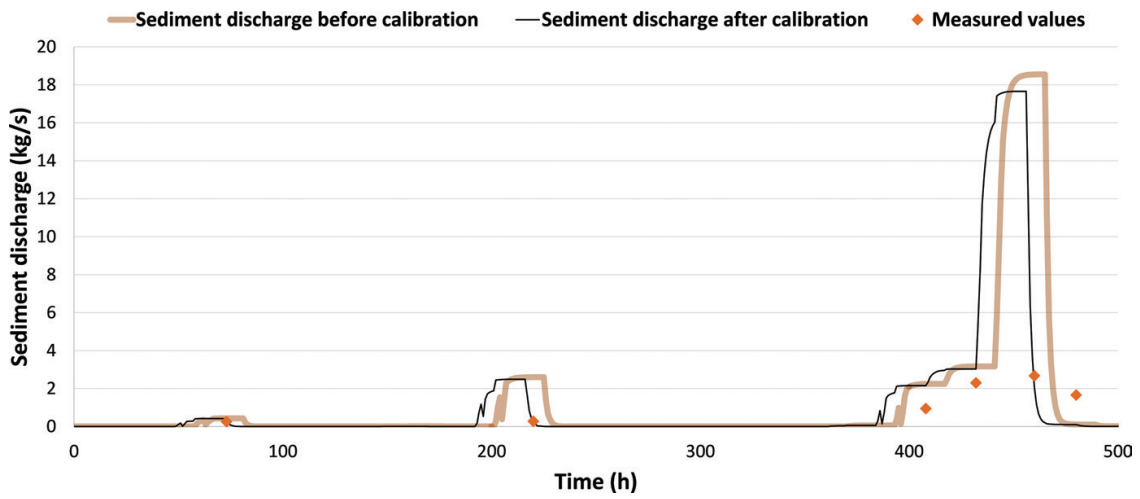

Figure 7. Sediment graph (April–May 2007, Kosynthos river basin outlet).
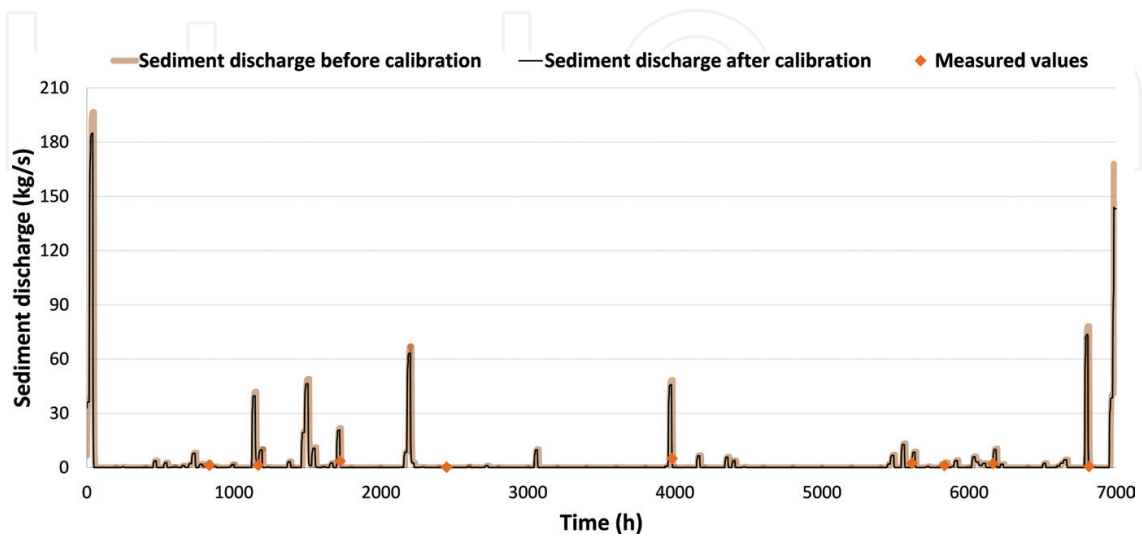

Figure 8. Sediment graph (April 2008–January 2009, Kosynthos river basin outlet).

As already mentioned, sediment discharge is mainly due to soil erosion, which in turn is a function of rainfall and runoff. Hence, the sediment discharge should be expected to be high when the discharge is high. Indeed, the sediment graphs follow a similar pattern with that of the hydrographs. High sediment discharges are observed in the same months as high water discharges, that is March, October, November and December. Sediment discharge also presents high values in January and May.

6.2. Nestos river basin

6.2.1. Water discharge

In **Figures 9** and **10**, the comparison between the computed discharge hydrographs for the two measurement sites used for the calibration of the model, Paschalia and Stavroupoli, before and after the calibration, is depicted. In **Figure 11**, the computed discharge hydrograph and the measured discharge values at Galani measurement site are depicted for the period March
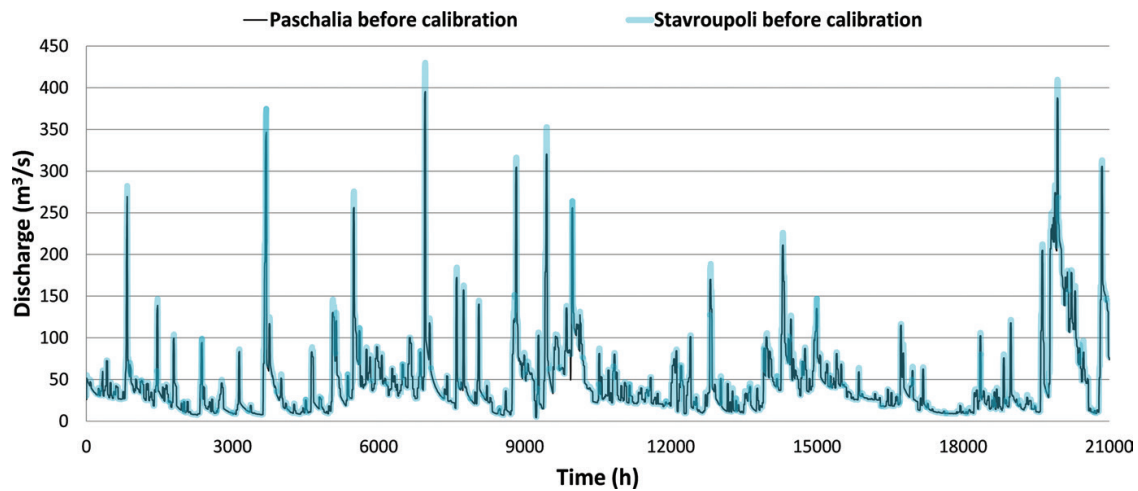

Figure 9. Discharge hydrograph (October 2006–March 2009, Paschalia-Stavroupoli before calibration).
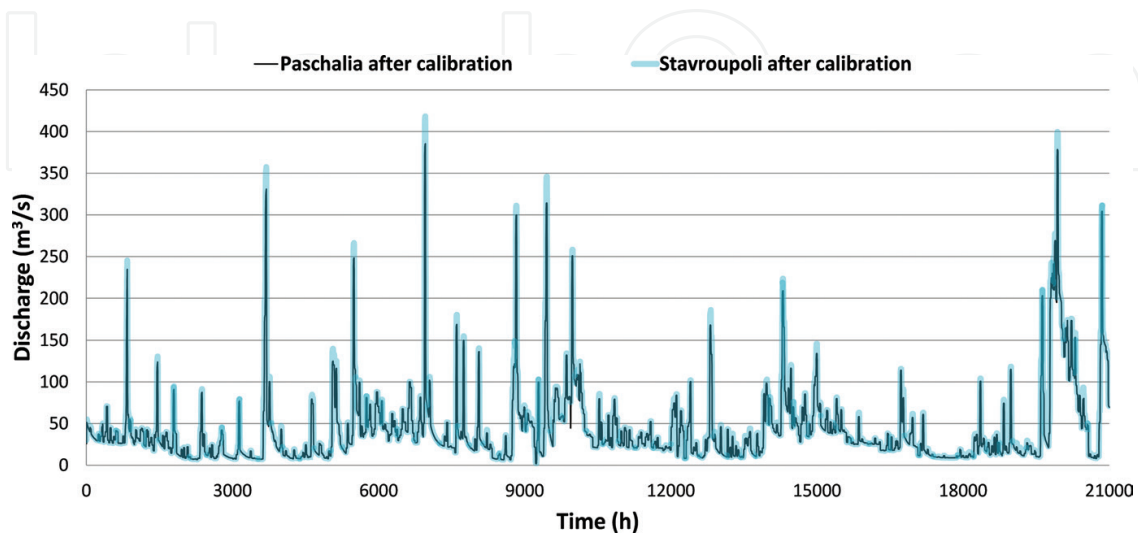

Figure 10. Discharge hydrograph (October 2006–March 2009, Paschalia-Stavroupoli after calibration).

2006–January 2009. In **Figures 12–15**, the computed discharge hydrographs and the measured discharge values at the basin outlet are depicted for the periods September–October 2005, July–November 2008, July 2009–January 2010 and March–May 2011.

As it can be observed from **Figures 9** and **10**, the hydrographs of the two upstream measurement sites follow the very same pattern, with exception that the discharge at Paschalia, which is located a little upstream from Stavroupoli, is slightly lower. Further downstream, at Galani measurement site, the discharges increase even more. This is due to the addition of more sub-basins and their hydrological distribution to Nestos River. Discharges higher than 200 m³/s are mostly observed in months January, March, October, November and December at the aforementioned measurement sites.

The case is different at the basin outlet, which is the final measurement site. Here, the presence of the two irrigation canals, which divert large volumes of water during the irrigation period, is a game-changing element as far as the discharge is concerned. The two canals irrigate the plains of Kavala and Xanthi. The irrigation period, in both cases, starts in April and goes up to
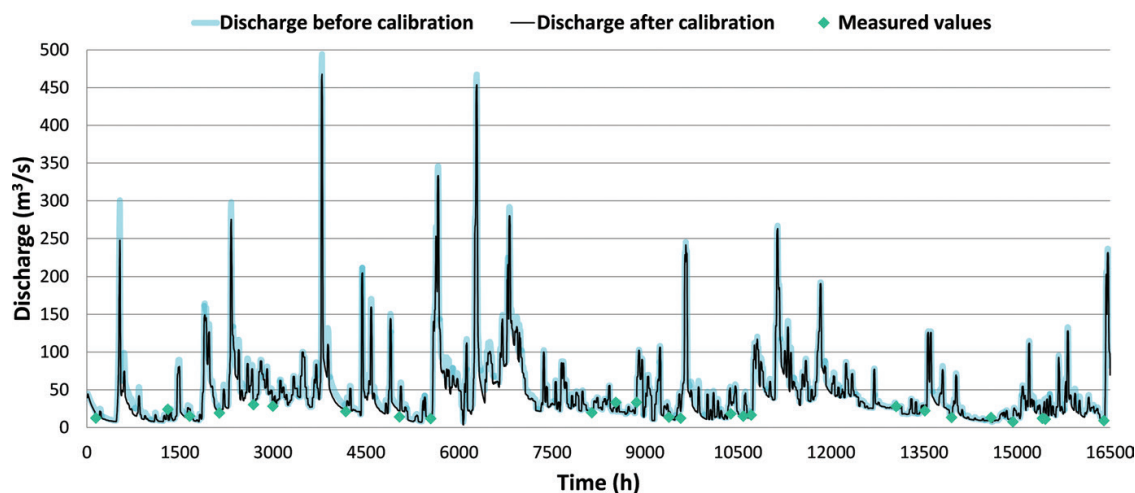

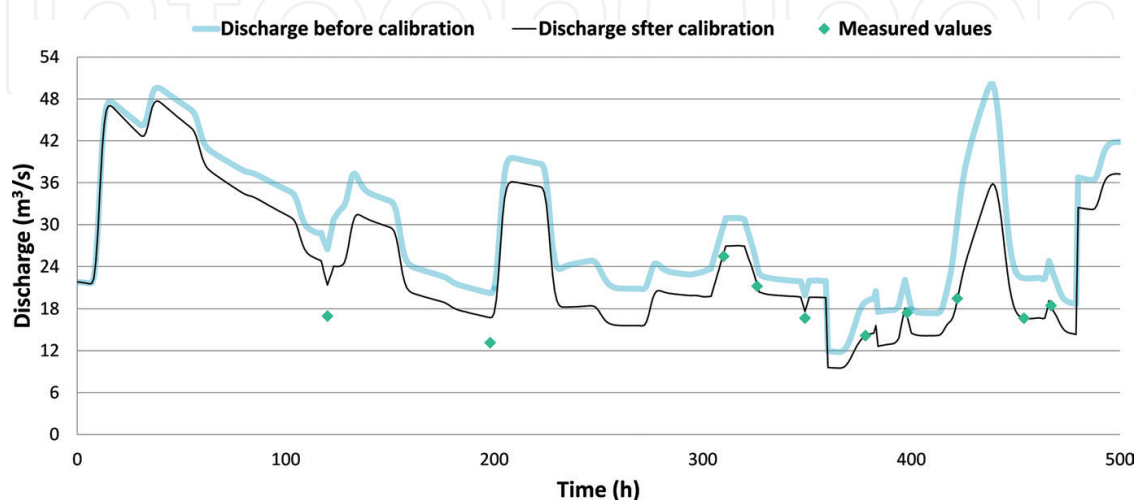**Figure 11.** Discharge hydrograph (March 2006–January 2009, Galani).

Figure 12. Discharge hydrograph (September–October 2005, Nestos river basin outlet).
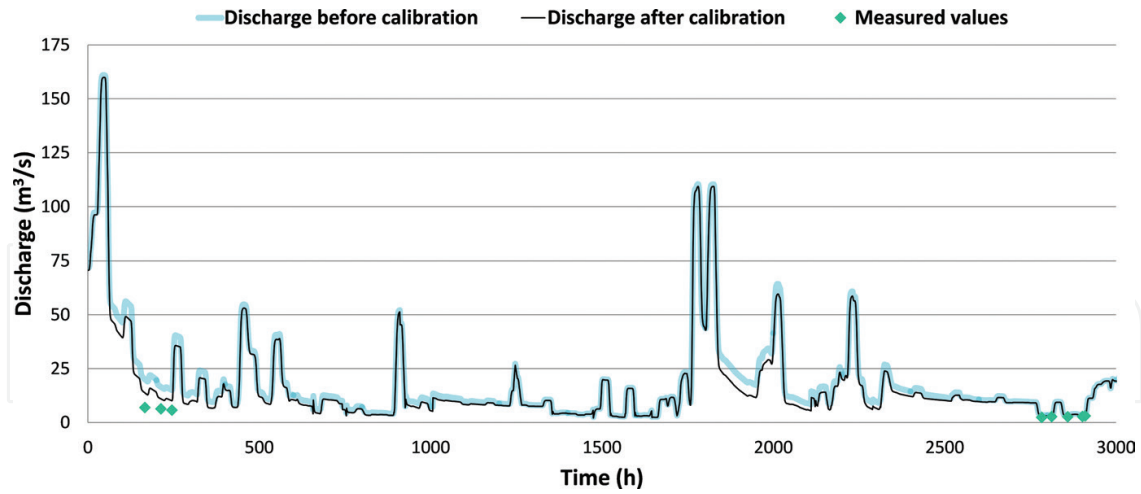
Figure 13. Discharge hydrograph (July–November 2008, Nestos river basin outlet).
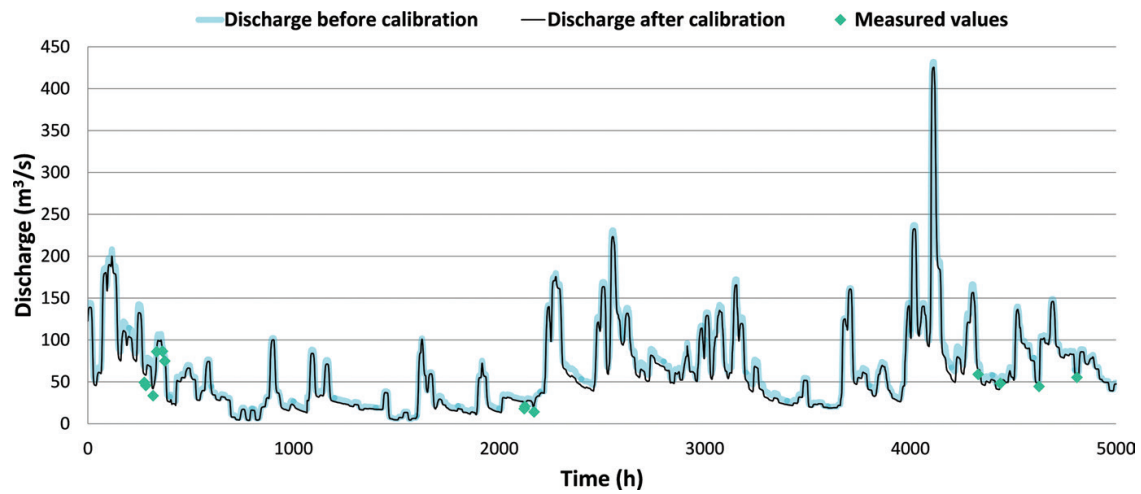

Figure 14. Discharge hydrograph (July 2009–January 2010, Nestos river basin outlet).
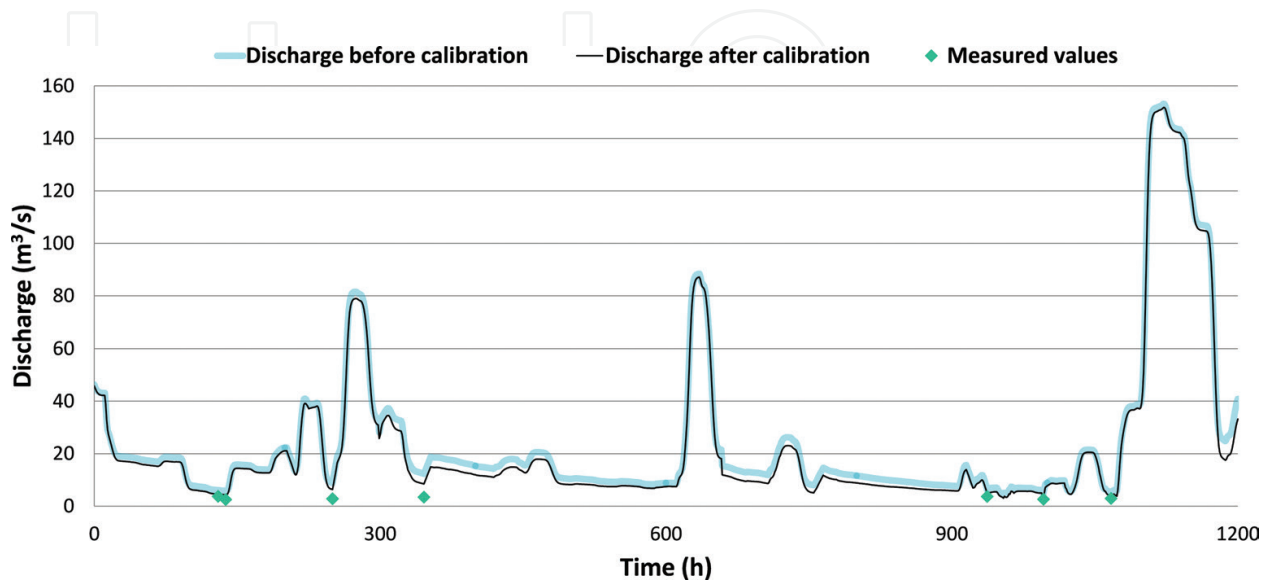

Figure 15. Discharge hydrograph (March–May 2011, Nestos river basin outlet).

October. The amount of water that gets subtracted from Nestos River is much higher during the drier months of the summer. Especially during this period, the Platanovrysi dam holds a vital role in the sustainability of the water resources management by replenishing the riverine system and by securing environmental flows.

6.2.2. Sediment discharge

In **Figures 16–18**, the computed sediment graphs (bed load + suspended load) at the basin outlet are illustrated for the periods September–October 2005, June 2008–June 2011 and October 2011–July 2014.

Despite the fact that the Platanovrysi dam hinders a portion of sediment, the basin itself provides the streams with the necessary amount of sediment that is vital for the aquatic ecosystems and for a variety of environmental reasons. The simulated sediment discharge reaches an overall average value of approximately 30 kg/s, whilst—as seen from **Figures 17** and **18**—there are several high peaks as well.
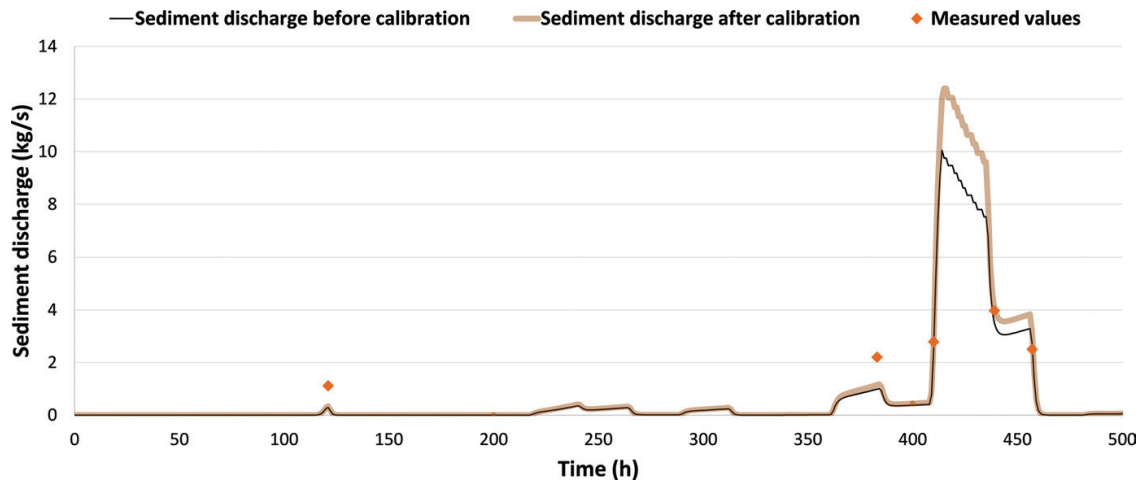

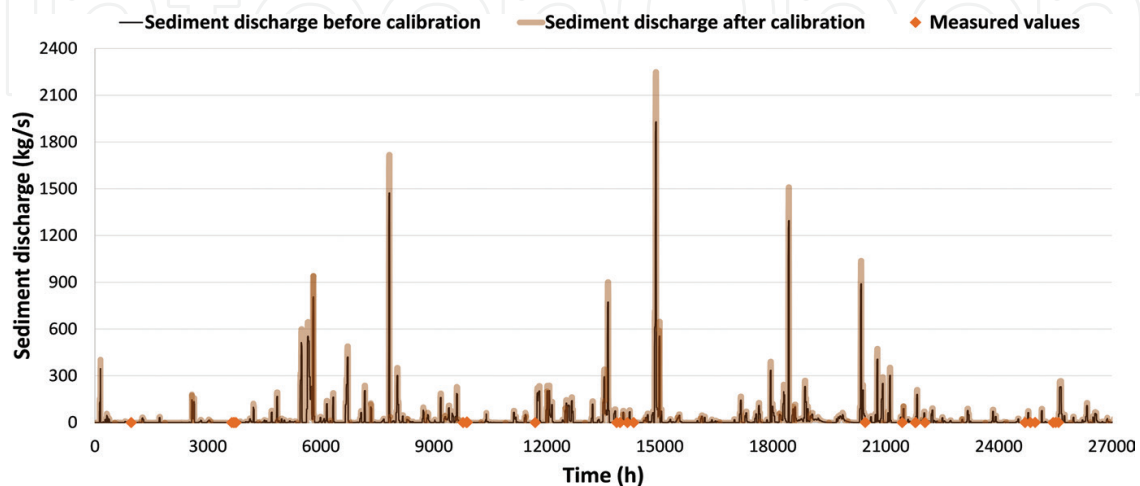**Figure 16.** Sediment graph (September–October 2005, Nestos river basin outlet).

Figure 17. Sediment graph (June 2008–June 2011, Nestos river basin outlet).
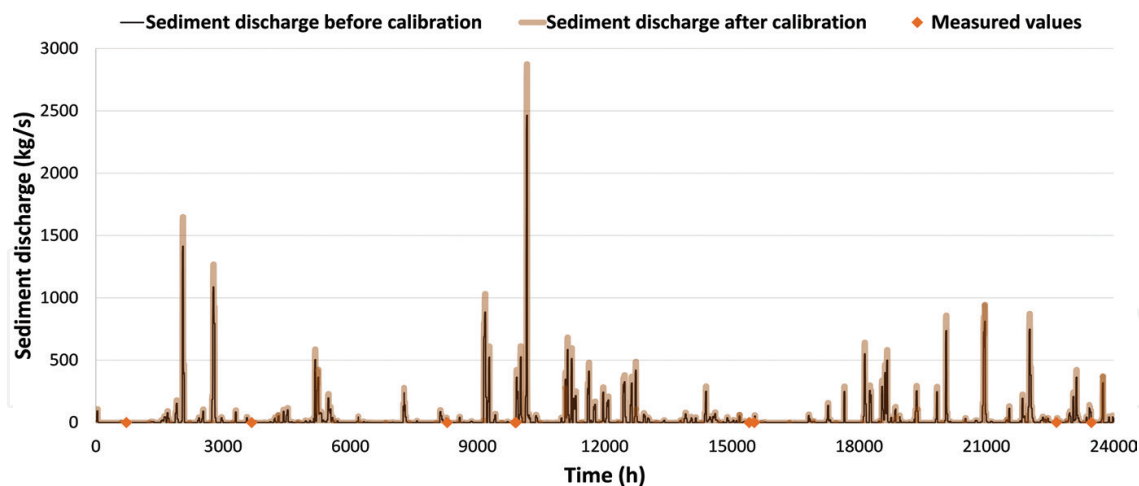
Figure 18. Sediment graph (October 2011–July 2014, Nestos river basin outlet).

6.3. Efficiency criteria

A series of efficiency criteria were used for the comparison between computed and measured water discharge and sediment discharge values. The criteria utilized, as well as their values, are shown in **Table 3**.

Efficiency criteria	Kosynthos river basin		Nestos river basin		
	Basin outlet		Galani	Basin outlet	
	Water discharge	Sediment discharge	Water discharge	Water discharge	Sediment discharge
Mean absolute error (m³/s, kg/s)	0.4062	0.4239	2.9332	2.4944	0.2876
Mean relative error (%)	7.5528	6.9342	20.0945	25.4658	12.3819
Mean square error (m⁶/ s², kg²/s²)	0.4984	0.5358	19.5876	14.9494	0.3829
Root mean square error (m³/s, kg/s)	0.706	0.732	4.4258	3.8665	0.6188
PBIAS (%)	−1.5411	−11.7108	−15.4909	−10.3444	12.3711
Nash-Sutcliffe efficiency	0.8641	0.5899	0.65	0.9737	0.6469
Index of agreement, d	0.9649	0.9096	0.9103	0.9936	0.8917
Coefficient of persistence	0.9006	0.7413	0.6627	0.9603	0.6413
Coefficient of performance	0.1359	0.4101	0.35	0.0263	0.3531
Correlation coefficient	0.9318	0.8485	0.8943	0.9925	0.8127
Determination coefficient	0.8682	0.7199	0.7997	0.985	0.6605
t-Test (P-value > 0.05)	0.9355	0.6781	0.1926	0.675	0.6866

Table 3. Efficiency criteria values.

The validation of a time series model, such as the one applied in the current study, is integrated by the use of appropriate statistic criteria of efficiency, which are applied for the comparison between calculated and measured values and determine whether a model is successful or not.

There is a wide range of literature on the efficiency criteria utilized in this study. Their formulas, theoretical concepts and efficiency ranges (**Table 4**) should be comprehended before one uses them.

Efficiency criteria	Range of efficiency
Mean absolute error (m^3/s, kg/s)	The closer to 0 (perfect fit) the MAE is, the closer the fit between observed and predicted values
Mean relative error (%)	The closer to 0 (perfect fit) the MRE is, the closer the fit between observed and predicted values. A (−) or a (+) indicates an underprediction or an overprediction of the model
Mean square error (m^6/s^2, kg^2/s^2)	The closer to 0 (perfect fit) the MSE is, the closer the fit between observed and predicted values
Root mean square error (m^3/s, kg/s)	The closer to 0 (perfect fit) the RMSE is, the closer the fit between observed and predicted values
PBIAS (%)	(−) indicates an overprediction of the model, whilst (+) indicates an underprediction of the model. The optimal value is (0). Satisfactory values according to Moriasi et al. [33]: streamflow = ±25% and sediment = ±55%
Nash-Sutcliffe efficiency	Efficiencies range from −Inf to 1, with 1 being the optimal value (perfect fit)
Index of agreement, d	The index of agreement ranges from 0 to 1, with 1 being the optimal value (perfect fit)
Coefficient of persistence	C_P ranges from 0 to 1, with 1 being the optimal value, whilst a value larger than 0 indicates a "minimally acceptable" model performance [34]
Coefficient of performance	The coefficient of performance approaches to 0 as the predicted values approach the observed ones
Correlation coefficient, r	$−1 \leq r \leq +1$. The + and − signs are used for positive and negative linear correlations, respectively. A perfect correlation of ± 1 occurs when all the data points lie exactly on a straight line
Determination coefficient, r^2	The range of r^2 lies between 0 and 1. A value of zero means no correlation at all, whereas a value of 1 means that the dispersion of the prediction is equal to that of the observation
t-Test (P-value > 0.05)	The acceptance or not of a t-test's result relies on whether a probability value (P-value) is greater or not than the significance level (alpha). Alpha was set to 0.05

Table 4. Efficiency ranges of the statistic criteria.

7. Discussion

The hydrologic model was calibrated under four parameters which regulate the surface runoff, as well as the baseflow and the total discharge. The decrease or the increase of

CN "constitutes" the soil surface more or less susceptible to infiltration by water and, therefore, leads to a proportionate reduction or increment of surface runoff. An increase of lag time enhances the infiltration process by "retaining" runoff for more time on the soil surface, augmenting the hydrologic losses this way. The decrease of lag time has the opposite effect.

The most influencing parameters of HEC-HMS, as far as baseflow and total stream discharge are concerned, were proved to be the baseflow recession constant and the flow ratio. These two parameters have a high and direct impact on baseflow and total discharge. However, they also constitute an indirect influence on the sediment transport in streams by affecting the stream sediment transport capacity.

Both sediment discharge and sediment yield are highly dependent on surface runoff. Surface runoff is the decisive parameter in soil erosion; the lower the runoff discharge is, the lower is the erosive force and the sediment transport capacity of the flowing water.

Soil cohesion plays a decisive role in soil erosion, hence, the calibration of the entrainment ratio. Generally, the lower the cohesion of the soil, the more easily the soil particles are rived and eroded.

A decrease of the streambed roughness coefficient leads to a decrease of the stream sediment transport capacity. This leads to channel deposition which, in turn, results in a decrease of sediment discharge at the basin outlet.

In the past, the annual sediment yield because of rainfall and runoff was computed at the outlet of Kosynthos river basin [35] and at the outlet of Nestos river basin [32]. However, in both cases, the computations were performed on a monthly basis.

8. Conclusions

It is concluded that there is a very good approximation between the computed and measured discharge and sediment discharge values and that the deviation between these values is not considerable.

According to Ref. [36], the full benefit of an erosion prediction model is gained through the use of a continuous simulation model. By continuous simulation, it is meant that the model follows the time variation of the physical processes related to erosion.

The combination of a hydrologic model with a soil erosion model and a stream sediment transport model enables the transition of the hydrograph, due to a rainfall event, at a basin outlet to the corresponding sediment graph. In other words, the variation with time of the sediment discharge at the basin outlet is computed on the basis of the variation with time of the stream discharge due to the rainfall event [37]. The continuous nature of the hydrograph enables the development of a continuous sediment graph. It could be stated that the connection of the models through the input-output data ensures the almost parallel running of the models, which approximates the natural reality.

It is believed that the deviations between computed and measured water discharge and sediment discharge values for single rainfall events can be mitigated by means of the continuous hydro-geomorphologic modelling because of the integrating effect obtained through the use of a long simulation period. Continuous hydro-geomorphologic modelling for a relatively long time period, in a relatively large basin, provides a more realistic representation of the runoff process, as well as the soil erosion and sediment transport processes.

Seeing that the overwhelming majority of rivers in Greece are ungauged, HEC-HMS can reliably be used to calculate stream discharges and simulate river flows across the country. It can also be applied to other parts of the Mediterranean, with similar morphological and climatic conditions. Additionally, given the fact that the process of measuring the sediment discharge is a difficult and laborious task—yet of great significance for a variety of reasons—the composite mathematical models presented here can be used in the Greek mountainous terrain to successfully estimate soil erosion, sediment discharges and sediment yields at the basin scale.

Finally, continuous simulation of the hydromorphological processes can be an indicator of the future trends concerning their quantification.

The results of the efficiency criteria conclude that the continuous hydro-geomorphologic modelling can be successfully applied to both Kosynthos river basin and Nestos river basin.

Author details

Konstantinos Kaffas* and Vlassios Hrissanthou

*Address all correspondence to: kostaskaffas@gmail.com

Department of Civil Engineering, Democritus University of Thrace, Kimmeria Campus, Xanthi, Greece

References

[1] Beasley DB, Huggins LF, Monke EJ. ANSWERS—A model for watershed planning. Transactions of the ASAE. 1980;**23**:938-944

[2] Merritt WS, Letcher RA, Jakeman AJ. A review of erosion and sediment transport models. Environmental Modelling & Software. 2003;**18**(8):761-799

[3] Holtan HN. A Concept for Infiltration Estimates in Watershed Engineering. Washington, DC: USDA-ARS Bulletin. 1961; pp. 41-51.

[4] Green WH, Ampt CA. Studies on soil physics, I. Flow of water and air through soils. Journal of Agricultural Science. 1911;**4**:1-24

[5] Wischmeier WH, Smith DD. Predicting Rainfall Erosion Losses: A Guide to Conservation Planning. In: Agriculture Handbook 282. 1400 Independence Ave., S.W., Washington, DC: USDA-ARS; 1978

[6] Yalin MS. An expression for bed load transportation. Journal of Hydraulics Division, ASCE. 1963;**98**(HY3):221-250

[7] Foster GR, Meyer LD. Transport of particles by shallow flow. Transactions of the ASAE. 1972;**15:**99-102

[8] Alonso CV, Nielberg WH, Foster GR. Estimating sediment transport capacity in watershed modeling. Transactions of the ASAE. 1981;**24:**1211-1220

[9] Young RA, Onstad CA, Bosch DD, Anderson WP. AGNPS, agricultural nonpoint source pollution. A watershed analysis tool. In: Conservation Research Report 35. Washington, DC: USDA; 1987

[10] Young RA, Onstad CA, Bosch DD, Anderson WP. AGNPS: A nonpoint-source pollution model for evaluating agricultural watersheds. Journal of Soil and Water Conservation. 1989;**44**(2):4522-4561

[11] Soil Conservation Service (SCS). National Engineering Handbook, Section 4: Hydrology. Washington, DC: USDA; 1972

[12] Renard KG, Foster GR, Weesies GA, McCool DK, Yoder DC. Predicting Soil Erosion by Water: A Guide to Conservation Planning with the Revised Universal Soil Loss Equation (RUSLE), Vol. 703. Washington, DC: US Government Printing Office; 1977

[13] Einstein HA. The Bed-Load Function for Sediment Transportation in Open Channel Flows. In: Technical Bulletin 1026. USDA; 1950

[14] Bagnold RA. Bedload transport in natural rivers. Water Resources Research. 1977;**13**(2): 303-312

[15] Knisel WG. CREAMS: A Field-scale Model for Chemicals, Runoff, and Erosion from Agricultural Management System. In: Conservation Research Report No. 26. Washington, DC: USDA-SEA; 1980

[16] Poesen J. An improved splash transport model. Zeitschrift für Geomorphologie. 1985;**29**: 193-211

[17] Yang CT, Stall JB. Applicability of unit stream power equation. Journal of the Hydraulics Division, ASCE. 1976;**102**(5):559-568

[18] Paschalidis G, Iordanidis I, Anagnostopoulos P. Discharge and sediment transport in a basin with a dam at its upper boundary. In: Proceedings of the 12th International Conference on Protection and Restoration of the Environment; 29 June–3 July 2014; Skiathos Island, Greece

[19] Global Weather Data for SWAT [Internet]. Available from: http://globalweather.tamu.edu/. [Accessed: 13 December, 2016]

[20] Thiessen AH. Precipitation averages for large areas. Monthly Weather Review. 1911;**39**(7): 1082-1089

[21] Allen RG, Pereira LS, Raes D, Smith M. Crop evapotranspiration: Guidelines for computing crop requirement, irrigation and drainage, Paper No. 56. Rome: FAO; 1998

[22] Giandotti M. Forecast from full and lean courses of water. Ministry LL.PP., Hydrographic Survey, Vol. 8, Rep. No. 2; 1934. Hydrographic Department of Italy, Rome (in Italian)

[23] Giandotti M. Empirical flood forecasting based on the meteoric precipitations, the physical and morphological characteristics of the basins; application of the method to some of the Ligurian basins. Memorie e Studi Idrografici. 1940;**10**:5-13 (in Italian)

[24] Pasini F. Report on the renana recovery plan. 1914; Bologna, Italy (in Italian)

[25] Soil Conservation Service (SCS). National Engineering Handbook, Section 4: Hydrology. Springfield VA: USDA; 1971

[26] Barnes BS. The structure of discharge recession curves. Transactions of the American Geophysical Union. 1939;**20**(4):721-725

[27] Cunge JA. On the subject of a flood propagation computatronal method (Muskingum method). Journal of Hydraulic Research. 1969;**7**(2):205-230

[28] United States Army Corps of Engineers (USACE). Hydrologic Modeling System HEC-HMS, User's Manual, Version 4.0. 2013; Hydrologic Engineering Center, Davis, CA

[29] Kaffas K, Hrissanthou V. Application of a continuous rainfall-runoff model to the basin of Kosynthos river using the hydrologic software HEC-HMS. Global NEST Journal. 2014;**16**(1):188-203

[30] Nielsen SA, Storm B, Styczen M. Development of distributed soil erosion component for the SHE hydrological modelling system. In: Proceedings of the International Conference on Water Quality Modelling in the Inland Natural Environment, BHRA; June 1986; Bournemouth, UK. pp. 1-13

[31] Engelund F, Hansen E. A monograph on sediment transport in alluvial streams. Copengahen: Teknisk Forlag; 1967

[32] Hrissanthou V. Comparative application of two erosion models to a basin. Hydrological Sciences-Journal-des Sciences Hydrologiques. 2002;**47**(2):279-292

[33] Moriasi DN, Arnold JG, Van Liew MW, Bingner RL, Harmel RD, Veith TL. Model evaluation guidelines for systematic quantification of accuracy in watershed simulations. Transactions of the ASABE. 2007;**50**(3):885-900

[34] Gupta HV, Sorooshian S, Yapo PO. Status of automatic calibration for hydrologic models: Comparison with multilevel expert calibration. Journal of Hydrologic Engineering. 1999;**4**(2):135-143

[35] Hrissanthou V, Delimani P, Xeidakis G. Estimate of sediment inflow into Vistonis Lake, Greece. International Journal of Sediment Research. 2010;**25**(2):161-174

[36] Lal R. Soil Erosion Research Methods. Soil and Water Conservation Society and St. Lucie Press, 6000 Broken Sound Parkway, NW, Boca Raton, FL; 1994

[37] Hrissanthou V, Theodorakopoulos E. Computation of sediment graph for a flood event. In: Proceedings 6th International Conference of the European Water Resources Association (EWRA); 2005; Menton, France; pp. 1-13